UC 34C+D

LBL-18320 c.1

Lawrence Berkeley Laboratory

UNIVERSITY OF CALIFORNIA

RECEIVED
LAWRENCE
BERKELEY LABORATORY

Physics Division

OCT 9 1984

LIBRARY AND
DOCUMENTS SECTION

Presented at the XXII International Conference on High Energy Physics, Leipzig, East Germany, July 19-25, 1984 and at PANIC, Particles and Nuclei - Tenth International Conference, Heidelberg, West Germany, July 30 - August 3, 1984

SEARCH FOR RIGHT-HANDED CURRENTS IN MUON DECAY

B. Balke, J. Carr, G. Gidal, B. Gobbi,
A. Jodidio, C.J. Oram, K.A. Shinsky, H.M. Steiner,
D.P. Stoker, M. Strovink, and R.D. Tripp

July 1984

For Reference

Not to be taken from this room

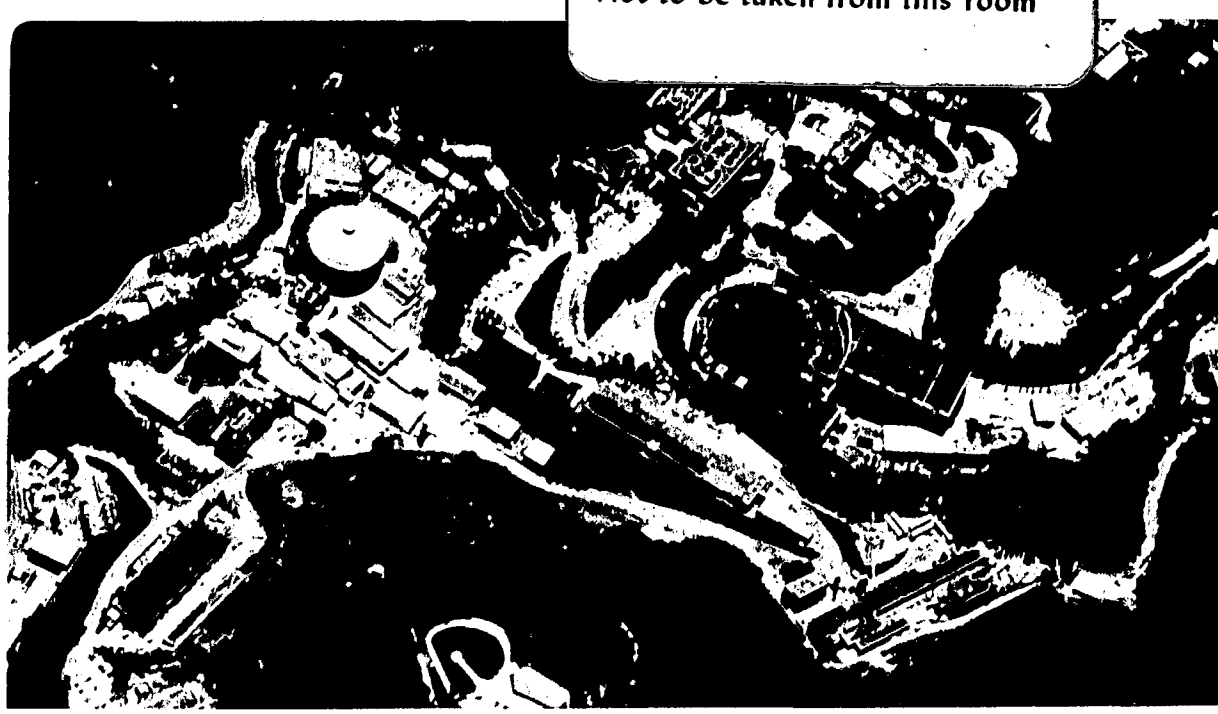

Prepared for the U.S. Department of Energy under Contract DE-AC03-76SF00098

LBL-18320 c.1

DISCLAIMER

This document was prepared as an account of work sponsored by the United States Government. While this document is believed to contain correct information, neither the United States Government nor any agency thereof, nor the Regents of the University of California, nor any of their employees, makes any warranty, express or implied, or assumes any legal responsibility for the accuracy, completeness, or usefulness of any information, apparatus, product, or process disclosed, or represents that its use would not infringe privately owned rights. Reference herein to any specific commercial product, process, or service by its trade name, trademark, manufacturer, or otherwise, does not necessarily constitute or imply its endorsement, recommendation, or favoring by the United States Government or any agency thereof, or the Regents of the University of California. The views and opinions of authors expressed herein do not necessarily state or reflect those of the United States Government or any agency thereof or the Regents of the University of California.

LBL-18320

SEARCH FOR RIGHT-HANDED CURRENTS IN MUON DECAY

B. Balke, J. Carr, G. Gidal, B. Gobbi*, A. Jodidio, C.J. Oram**,
K.A. Shinsky†, H.M. Steiner, D. P. Stoker, M. Strovink, and R.D. Tripp

Lawrence Berkeley Laboratory and Department of Physics
University of California
Berkeley, California 94720, U.S.A.

*Department of Physics
Northwestern University
Evanston, Illinois 60201, U.S.A.

**Tri-University Meson Facility
Vancouver, BC, V6T2A3, Canada

(represented at Conference by H.M. Steiner)

Presented at:

XXII International Conference on High Energy Physics
Leipzig, GDR, July 19-25, 1984

PANIC, Particles and Nuclei - Tenth International Conference
Heidelberg, West Germany, July 30-August 3, 1984

†Deceased.

ABSTRACT

The parameter ξ, which characterizes the anisotropy of the emitted electrons relative to the spin direction of the muon, is a sensitive indicator of possible $V+A$ admixtures to the dominant $V-A$ weak interaction responsible for muon decay. We report here new results relating to the measurement of ξ based on an experiment performed with a highly polarized surface muon beam at the TRIUMF cyclotron. The muons were stopped in thin metal foils in order to minimize depolarization effects. A spectrometer consisting of magnets and position sensitive detectors was tuned to accept electrons near the end point of the decay spectrum. Two largely independent methods were used to determine ξ. In the first we measured the rate of positrons emitted in a direction opposite to the muon's spin as a function of their momentum when the stopping target was immersed in a 1.1 T longitudinal magnetic field. In the second method the stopping muons were subjected to a weak transverse magnetic field and the amplitude of their spin precession oscillation was used to determine ξ. Based on the results from both methods lower limits on the mass of an intermediate vector boson which couples to right-handed weak currents are 400 GeV/c^2 when no constraints are placed on $W_L - W_R$ mixing and 470 GeV/c^2 if mixing is assumed to be absent. These limits represent about an order of magnitude improvement over those obtained from previous measurements of ξ. We have used the same apparatus to measure the anisotropic shape parameter δ. Preliminary results are consistent with the expected value of 3/4 with errors that are a factor of two smaller than previous measurements.

I. Introduction

The standard model of electroweak interactions,[1-3] based on the gauge group U(1) $\times$ $SU(2)_L$, has been remarkably successful in describing experimental observations. The question of why electroweak processes are left-handed is not addressed by this model, but rather the left-handedness is built in a priori. It is possible to restore left-right symmetry at the Lagrangian level in a way that is consistent with the very obvious experimental fact that weak processes are dominantly left-handed, by invoking the gauge group U(1) $\times$ $SU(2)_L$ $\times$ $SU(2)_R$ with the additional assumption that the left-right symmetry is spontaneously broken in a way that strongly suppresses right-handed effects.[4] As a consequence the mass of the right-handed gauge boson, W_R, would have to be greater than that of the left-handed gauge boson, W_L, by an amount which is large compared to M_{W_L} but which could be tiny on the grand unification mass scale of 10^{15} GeV. Actually the mass eigenstates, W_1 and W_2, are in general expressible as linear combinations of the gauge boson states, W_L and W_R:

$$W_1 = W_L\cos\zeta - W_R\sin\zeta$$

$$W_2 = W_L\sin\zeta + W_R\cos\zeta$$

where ζ is a mixing angle.

The effects of $W_L - W_R$ mixing and W_1 exchange relative to W_2 exchange become independent of momentum transfer for $q^2 \ll M^2(W_1)$. Analyses of muon and nucleon β decay which neglect the kinematic effects of possible finite ν_R mass have yielded the strongest limits on the mass-squared-ratio $\alpha = M^2(W_1)/M^2(W_2)$ and on ζ.[5,6] Additional constraints are placed by model-dependent calculations of the $K_L - K_S$ mass difference[7-10] and by current-algebra relations between $K\to3\pi$ and $K\to2\pi$ amplitudes.[11]

The present experimental bounds[12-17] are displayed as contours in Figure 1. The small bold contour is derived from the experiment described in this paper.

The main emphasis in this experiment has been on measuring the asymmetry parameter, ξ, in muon decay by observing the decay of highly polarized μ^+ stopped in

pure metal foils. The target material was chosen to minimize depolarization effects. The decays of interest are those which emit e^+ near the momentum spectrum endpoint $x = p_e/p_e(\max) \sim 1$. The use of a highly polarized "surface muon" beam together with the measurement of the endpoint spectrum with a high resolution spectrometer has allowed us to achieve an order of magnitude improvement in sensitivity over the best previous search for V+A effects in muon decay.[18]

Neglecting radiative corrections and assuming massless neutrinos the μ^+ differential decay rate is

$$\frac{d^2\Gamma}{x^2 dx d(\cos\vartheta)} \propto \left[(3-2x) + (\frac{4}{3}\rho - 1)(4x-3) + 12\frac{m_e}{m_\mu}\frac{x-1}{x}\eta\right] - \left[(2x-1) + (\frac{4}{3}\delta - 1)(4x-3)\right]\xi P_\mu \cos\vartheta. \quad (1)$$

Here $\pi-\vartheta$ is the angle between the momentum, $\vec{p}_e$, of the outgoing positron and the polarization, P_μ, of the stopped muon. The four muon decay parameters are tabulated in Table 1 together with their expected values from the V-A theory and the 1982 experimental values.

Table 1. Muon decay parameters

Parameter	V-A Value	Experiment
ρ (isotropic shape)	3/4	0.7517 ± .0026
δ (anisotropic shape)	3/4	0.755 ± .009
η (low energy parameter)	0	-0.12 ± .21
ξ (asymmetry parameter)	1	0.972 ± .014

At the endpoint (x = 1) Eq. (1) reduces to

$$\frac{d^2\Gamma}{dx d(\cos\vartheta)} \approx 1 - \frac{\delta\xi}{\rho} P_\mu \cos\vartheta. \quad (2)$$

Thus deviations of the quantity $\frac{\delta\xi P_\mu}{\rho}$ from its V-A value of 1 result in a non-vanishing rate of decay positrons at x = 1 and $\cos\vartheta = +1$. The connection to intermediate vector

boson masses and mixing angles is made by noting that $1-\frac{\delta\xi P_\mu}{\rho} \sim 2(2\alpha^2 + 2\,\alpha\,\zeta + \zeta^2)$ when both $\alpha << 1$ and $\zeta << 1$.

Figure 2 shows the expected momentum spectrum of positrons produced from decays at rest of completely polarized muons when the positrons are emitted, as in our experiment, opposite to the muon spin direction. This is displayed both for the case where the decay is mediated by a left-handed current V-A and by a right-handed current V+A. Also shown is the momentum spectrum for the decay of unpolarized muons. These curves could equally well be labeled, for the V-A case and complete polarization, as $\cos\vartheta = +1, -1, 0$ respectively. Thus labeled, they are plots of Eq. 1 for $\rho = \delta = 3/4$, $\eta = 0$, $\xi = P_\mu = 1$. In addition 1st and 2nd order radiative corrections are included in these curves. The thickened line of Figure 2 indicates the region of x and $\cos\vartheta$ covered by this study.

We have measured the quantity $\xi P_\mu \delta/\rho$ in two ways. In the first method the shape of the spectrum is measured near the vanishing end-point with the spin held by a 1.1 T longitudinal magnetic field. The second method is a muon spin rotation (μSR) experiment in which the muon spins are precessed by either a 70 G or a 120 G transverse field. The decay asymmetry is then extracted from the amplitude of the resulting μSR signals. Results obtained with the second method have slightly larger statistical errors than the spin-held results but are otherwise comparable in precision. In our most recent run we have used the μSR method to measure also the anisotropic shape parameter δ by extending the μSR measurements near x = 1 downward to well below x = 0.5 where, as can be seen from Fig. 2, the asymmetry changes sign.

II. Experimental Method

This experiment is made possible by the nearly complete polarization of a μ^+ beam derived from π^+ decay at rest near the surface of the production target.[19] Muons from π^+ decay deeper inside the production target have lower momentum and are less polarized due to Coulomb scattering. By tuning the beam line to the surface muon edge (Figure 3) we select the most highly polarized muons. When 100 μA of 500 MeV protons are incident on a 2 mm thick carbon target the M13 beam[20] at TRIUMF produces 15,000 μ^+/sec of 29.5 MeV/c within a 1% momentum bite and a 12 × 10 mm spot. The 2% contamination of prompt ("cloud") μ^+ from π^+ decay in flight near the production target is less polarized and is rejected by requiring the μ^+ to be produced well within the 43 nsec interval between proton bursts. A smaller π^+ flux is similarly rejected. Positrons in the beam constitute about 50% of the total flux; however, they pass through the μ stopping target and do not satisfy the trigger requirements.

The apparatus is shown in Figure 4. After traversing 50 mg/cm^2, the muons in the beam are stopped by target foils of ≥99.9% pure Al, Cu, Ag, and Au. The high free electron concentration in these metals screens the stopped μ^+ from prolonged spin-spin coupling to particular electrons, which otherwise would lead to its depolarization. A 1.1 T longitudinal field (B_L) is also applied to preserve the stopped μ^+ spin direction. During alternate hourly runs the longitudinal field is nulled and either a 70 gauss or a 120 gauss transverse field (B_T) is substituted. This precesses the μ^+ spin about a vertical axis so that its time-averaged polarization is zero.

The incoming μ^+ direction is determined using proportional chambers P1 and P2, and the outgoing e^+ direction is determined by proportional chamber P3 and drift chambers D1 and D2. Downstream of the target the decay e^+ is focused by a 0.5 T-m solenoidal field lens. The septum between the target and solenoid bore essentially decouples the focal length from the choice of target field orientation.

The decay e^+ is momentum-analyzed by an NMR-monitored cylindrical dipole magnet having a central field of 0.32 T. Low mass drift chambers are located near its conjugate foci and the intervening volume is evacuated. The momentum dispersion was measured to be 1.07%/cm by passing e^+ beams of different momenta, determined using the NMR-monitored beam line dipoles, through the spectrometer. The combined system of field lens and positron spectrometer has an acceptance of 250 msr and a momentum bite of ±20%; in the analysis described below these are restricted to 160 msr and ±12%.

The trigger requires the signature of a beam particle stopping in the foil target, in delayed (0.2 - 10 μs) coincidence with that of a decay positron passing through the spectrometer. Events with an extra beam particle arriving between the μ-stop and decay are tagged and rejected later.

Incoming μ^+ tracks were reconstructed using P1 and P2. Nearly straight e^+ track segments were found separately in the horizontal and vertical projections of three groups of wire chamber planes: P3, D1, D2; D3; and D4 (Fig. 4). All possible combinations of hits were considered, and tracks in all six segments were found in 99% of the triggers. Of these, 95% had multiplicities corresponding to a single track; the remainder were rejected. Projections of the track segments were required to agree at the target, in the bore of the solenoid, and in position and vertical slope in the spectrometer. The first of these requirements rejects most of the remaining small fraction of events where the e^+ is emitted from a μ^+ other than the current μ-stop. Track segment residuals were used to dynamically fine-tune the drift-chamber space-time calibration, producing residuals of $\leq$250 μm in the spectrometer chambers D3 and D4.

The hits found in P1 through D2 were then fitted to curved trajectories based on the first-order optics of cylindrically symmetric fields. The μ^+ and e^+ polar angles ϑ_μ and ϑ_e with respect to the beam axis were thereby determined with resolutions of 20 and 10 mrad respectively. Monte Carlo simulation based on higher-order field optics

confirms the accuracy of this procedure to within an uncertainty of ± 0.0005 in $\cos \vartheta_\mu$ and $\cos \vartheta_e$. In the presence of the longitudinal holding field the transverse component of the μ^+ spin precesses about the beam axis too rapidly to be followed. Thus for $\cos \vartheta = -\hat{P}_\mu \cdot \hat{p}_e$ in (2) we substitute $\cos \vartheta_\mu \cos \vartheta_e$, which is equivalent in an average over many events.

The e^+ momentum was obtained, to first order, from the measured dispersion and the sum of the horizontal coordinates at the conjugate foci of the 98° horizontally focusing spectrometer magnet. Empirical corrections to second order, based primarily on the end point position for the B_T data, were made for deviation from the median plane and impact parameter with respect to the magnet axis. The sharp edge at x=1 in Figure 5 curve (a) exhibits a gaussian resolution which is less than 0.2% rms, with a rounded shoulder due to non-uniform energy loss in the stopping target and the other materials upstream (~ 190 mg/cm^2).

In the μSR analysis we have excluded events with $x < 0.88$ or $\cos \vartheta_e < 0.975$ which have low statistical power for determining the decay asymmetry. For the spin held data the corresponding cuts are $x > 0.92$ and $\cos \vartheta > 0.975$. After conservative fiducial cuts the final distributions in Figure 5 retain 7.5% of the raw triggers. We have checked that any reasonable variation of the cuts would negligibly affect the result.

III. Results

A. SPIN-HELD DATA

Fitting proceeds in two stages. The B_T data in Fig. 5(a) are fitted to the radiatively corrected spectrum expected for unpolarized μ^+ decay, smeared by a sum of gaussian resolution functions and by the expected e^+ energy-loss straggling. The fit simultaneously calibrates the edge position x = 1 and determines the momentum resolution and the (quadratic) dependence of the acceptance upon x. The B_L spectrum in Figure 5b can be represented as the shape expected from pure (V-A) and $P_\mu = \cos\vartheta = 1$, with a small admixture of the unpolarized spectrum in Figure 5a. This unpolarized fraction is essentially equal to $1 - (\xi P_\mu \delta/\rho)\langle\cos\vartheta\rangle$. To fit this fraction, we use the B_T fit to fix the x resolution, x acceptance, and edge position x=1, but allow the acceptance for B_L data relative to that for B_T data to vary linearly with x. This allows for the (<2%) difference in angular acceptance caused by the different field configuration near the target. Using data with partly polarized cloud μ^+, we have checked that the x=1 calibration is consistent for B_L and B_T fields. In the resulting curve in Figure 5b, the slight kink near x = 1 reflects the unpolarized fraction, which arises mostly from the measured value $\langle\cos\vartheta\rangle = 0.9862$ for these data.

The result reported here is based on this same fitting procedure carried out for data in each of five bins in $\cos\vartheta$. The subdivision checks that the results of these fits are consistent with a linear dependence on $\langle\cos\vartheta\rangle$. The value of $\xi P_\mu \delta/\rho$ is determined by making a fixed slope extrapolation to $\cos\vartheta = 1$ (see Figure 6). Separate fits for each of the four stopping target materials (see Figure 7) give values of $\xi P_\mu \delta/\rho$ which are statistically consistent ($\chi^2 = 2.1$), with a combined statistical error of ± 0.0015. Within statistical errors the result is also independent of the time of muon decay.

Multiple Coulomb scattering in the production and stopping targets causes a misalignment of the μ^+ spin and momentum, resulting in the measured values of cos ϑ_μ being systematically too large. An estimated correction of +0.0012 ± 0.0005 is made to $\xi P_\mu \delta/\rho$. Table 2 summarizes the major sources of systematic error.

Table 2

Major sources of systematic error and their estimated contributions.

Source of systematic error	Error
Coulomb scattering in targets	±0.0005
Correction of ϑ_μ and ϑ_e for bending in B_L field at target	±0.0010
Smearing of ϑ_μ and ϑ_e due to detector resolution and scattering	±0.0006
Possible shift in ϑ_e due to random hits and inefficiencies in D1 and D2	±0.0005
Method of averaging $\langle\cos\vartheta\rangle$	±0.0004
Difference in x = 1 edge calibration between B_T and B_L data	±0.0008
Normalization of B_L relative to B_T data	±0.0007

All other sources contribute $<10^{-4}$. In principle the systematic errors should be uncorrelated; in quadrature they add to ±0.0018. The resulting value is $\xi P_\mu \delta/\rho$ = 0.9989 ± 0.0015 (statistical) ± 0.0018 (systematic). We have made no correction for unknown sources of μ^+ depolarization either along the beam or in the stopping target. Since such effects can only decrease the apparent result, we therefore quote the limit:

$$\xi P_\mu \delta/\rho > 0.9959 \qquad \text{(90\% confidence)}$$

This result, which has been reported previously,[21] is based on an analysis of data taken during the first of three runs at TRIUMF. Since that time we have accumulated

more data and have made further investigations of possible systematic effects. These studies are still in progress and final results with somewhat smaller errors are expected soon. Two aspects of this work deserve special mention. One is a complete Monte Carlo simulation of the experiment which has already shown that our method of analysis seems to have no systematic biases. The second involves the accumulation of data with a weaker longitudinal holding field (B_L = 0.3 Tesla). These data will be used to look for unexpected depolarization effects and to cross check our momentum and acceptance calibrations.

B. μSR DATA

The B_T data can be used for a largely independent measurement of the decay asymmetry.

Maximum likelihood fits using Poisson statistics are made to a total of 4.3×10^5 B_T events and 1.3×10^6 B_L events in 243 time bins. For the B_L data, the expected number of events in each time bin is given by:

$$N_L(t) = N_L^0 \exp(-t/\tau_\mu) + C_L \tag{3}$$

The fitted background, C_L is consistent with zero. The fitted muon lifetime, τ_μ, is used in the fits to the B_T data.

The B_T data for each target foil and transverse field strength (70 G or 120G) are fitted in six x bins, each 0.02 wide, to the radiatively corrected and energy loss straggled differential decay rate, assuming (V-A) values for the muon decay parameters η, ρ, and δ. The background is assumed to be zero, as is found for the B_L data. The expected number of events in each time bin is then given by:

$$N_T(t) = N_T^0\left[\int_x A(x)dx + R(t)\langle\cos\vartheta\rangle_t \xi P_\mu \int_x B(x)dx\right]\exp(-t/\tau_\mu) \tag{4}$$

where A(x) and B(x) are the angle independent and angle dependent parts of the differential decay rate respectively; $\langle\cos\vartheta\rangle_t$ is the value of $-\hat{P}_\mu(t)\cdot\hat{p}_e$ appropriate to the particular time bin; and

$$R(t) = \exp(-\sigma t^2) \tag{5}$$

is a Gaussian relaxation function describing the time-dependent muon depolarization in the target foil.

The $\langle\cos\vartheta\rangle_t$ are determined from the observed μ^+ and e^+ track directions at the stopping target over a large interval of the B_T data time spectrum for which the decaying muons are, on average, unpolarized. Since the decay of unpolarized muons is isotropic, the observed angular distribution of the e^+ in these events is determined only by the acceptance of the apparatus. Similarly, the observed angular distribution of the incoming μ^+ is determined only by the acceptance of the apparatus and the beam phase-space. We allow the muon spin precession rate to be a free parameter in the fit which permits us to make an unbiased determination of $\langle\cos\vartheta\rangle_t = -\hat{P}_\mu(t)\cdot\hat{p}_e$ for each time bin by calculating the average $\cos\vartheta$ for every precessed μ^+ spin direction combined with every outgoing e^+ direction. The resulting fit, with the muon life-time dependence removed, is shown in Figure 8 superimposed on the combined data obtained using the aluminum and gold foils in a 70 G transverse field.

We make corrections totaling +0.0013 for μ^+ multiple Coulomb scattering upstream of the target foil, decay e^+ scattering prior to measurement of $\hat{p}_e$, and possible incomplete nulling of the longitudinal field in the target foil region. The resulting value $\xi P_\mu\delta/\rho = 0.9977 \pm 0.0019$ (statistical) $\pm$ 0.0012 (systematic) is consistent with the value obtained from the spin-held data. The corresponding 90% confidence limit is $\xi P_\mu\delta/\rho > 0.9948$.

Although we are confident that the μSR results presented here are essentially correct and that they are unlikely to change significantly, there are a few remaining features of these data which are still under study. For example we find that the values of $\xi P_\mu\delta/\rho$ taken with both thin and thick copper targets are systematically low compared to aluminum and gold. We attribute this effect to an as yet unknown muon depolarization mechanism in the Cu targets. It should be remembered that the copper results shown in Figure 9 do not weaken our quoted limits on right-handed currents

which are based only on data taken with the Al and Au targets. We are also making more detailed studies of the absolute momentum calibration of our spectrometer in an attempt to further reduce the systematic errors attributable to this source.

C. PRELIMINARY RESULTS ON δ

During our last run in January 1984 the same apparatus was used to make an improved measurement of the anisotropic shape parameter δ. Data were taken over a wide range of x values with aluminum targets of two thicknesses and with two different μSR precession frequencies. The results are very sensitive to the detailed x calibrations and to radiative effects. Much beam time was spent in thoroughly studying these systematic effects. A preliminary analysis of the asymmetry as a function of x is shown in Figure 10. Both the V-A theory and the left-right symmetric theory predict $\delta = 3/4$, but mixtures of scalar, pseudoscalar and tensor couplings can cause deviations from this value.

In the absence of radiative effects the asymmetry is expected to change sign when $x = 0.5$; however, internal and external bremsstrahlung causes the zero asymmetry point to shift to somewhat lower values of x. Our preliminary result is

$$\delta = 0.748 \pm 0.004(\text{statistical}) \pm 0.003(\text{systematic})$$

Ultimately we expect to reduce the combined statistical and systematic errors to the ± 0.003 level. Already the error on the present preliminary result is half of that of the best previous measurement.[22]

IV. Discussion and Conclusions

We summarize here the present limits on right-handed current effects in muon decay by combining the spin-held and spin-precessed results discussed in the previous sections. We find that $\xi P_\mu \delta/\rho \geq 0.9966$ at the 90% confidence level. The corresponding limits on the mass and mixing parameters, α and ζ, are represented by the small bold contour in Figure 1. If no constraints are placed on the value of the mixing angle ζ, $M_{W_R} > 400$ GeV/ c^2 (90% CL), whereas $M_{W_R} > 470$ GeV/ c^2 (90% CL) if ζ is set equal to zero. Equivalently, the V+A amplitude is less than 0.029 times the usual V-A amplitude in the limit of no left-right mixing. A comparison of this result to the earlier measurements of Akhamanov et al.[18] is shown in Figure 11. It should be noted that the limits reported here are conservative in that any uncorrected depolarization effects would tend to mimic right-handed contributions and thus make it appear as though the role of the V+A interaction is stronger than it actually is. It is also important to point out that our limits are only relevant if the mass of the associated right-handed neutrino is less than about 10 MeV/c^2.

We have so far restricted the discussion to V and A couplings only. A more general analysis can be made which admits S, P, and T terms as well. As pointed out recently by Mursula, Roos and Scheck,[23] a precision measurement of ξP_μ together with the determination of the μ^+ helicity in π^+ decay can be used to improve substantially the limits on possible S, P, and T couplings. In addition, an important new constraint is imposed by the improved δ parameter measurement. The exact nature of the S, P, and T limits depends on the assumptions and the method of analysis. For example one can write the most general four-fermi interaction for muon decay

$$L_{int} = -\frac{G}{\sqrt{2}} \sum_{i=1}^{5} [(\bar{e}\Gamma_i \nu_e)(\bar{\nu}_\mu \Gamma_i (G_i + G_i'\gamma_5)\mu) + \text{hermitian conjugate}]$$

$$\text{where } \Gamma_i = 1, \gamma_\lambda, \sigma_{\lambda\kappa}, \gamma_\lambda\gamma_5, i\gamma_5.$$

This leads to the following relations between $\frac{\xi\delta}{\rho}$ and the G_i and G_i' for the special cases

of scalar or tensor admixtures to the dominant V-A interaction:

(1) (V-A) + Tensor: $$\frac{\xi\delta}{\rho} \approx 1 - \frac{(G_T + G_T')^2}{8}$$

(2) (V-A) + Scalar + Pseudoscalar: $$\frac{\xi\delta}{\rho} \approx 1 - \left[\frac{(G_s - G_p')^2 + (G_s' - G_p)^2}{16}\right]$$

Hence from our result $\frac{\xi\delta}{\rho} \geq \frac{\xi P_\mu \delta}{\rho} > .9966$ we obtain the 90% confidence limits

$$(G_T + G_T')^2 < 0.027$$

$$(G_s - G_p')^2 + (G_s' - G_p)^2 < 0.054.$$

Mursula et al.[23] have obtained more stringent limits by making a global analysis based on all previously available data. With the inclusion of the results reported here significant additional improvements can be expected.

Our measurement of the vanishing endpoint of the momentum spectrum of positrons emitted opposite to the muon spin direction can be used to set a limit on flavor family symmetry breaking, assuming a model proposed by Wilczek.[24] In this model the breakdown of family symmetries involves characteristic massless axion-like Nambu-Goldstone bosons $f_{\ell\ell'}$ (familons) which couple to the divergences of currents which change flavor quantum numbers. The decay $\mu \to e + f$ would then occur with a branching ratio $\Gamma(\mu \to e + f)/\Gamma(\mu \to e\nu\bar{\nu}) = 2.5\times10^{14}(\mathrm{GeV})^2/F_{\mu e}^2$ where $F_{\mu e}$ is the energy scale at which the flavor symmetry is spontaneously broken. Because the decay $\mu \to e + f$ is isotropic its presence would be signaled by a spike in the positron momentum spectrum at x = 1. A fit of the spin-held data yields the limit $\Gamma(\mu \to ef)/\Gamma(\mu \to e\nu\bar{\nu}) = 6\times10^{-6}$ which implies that $F_{\mu e} \geq 6.5\times10^9$ GeV (90% CL).

The possibility that leptons and quarks are composite at some mass scale Λ has received considerable attention in recent years. Among the strongest experimental limits on Λ currently quoted[25,26] are those from Bhabba scattering (>750 GeV), muon (g-2) (>860 GeV), and a more model-dependent estimate from ν-hadron scattering (>2.5 TeV).

The effects of compositeness may be analyzed in terms of new effective contact interactions. Following the analyses of Peskin,[27] and Lane and Barany,[28] the most general SU(2) × U(1) invariant contact interaction contributing to $\mu \to e\nu\bar{\nu}$ is

$$\begin{aligned} L_{cont} = (g^2/\Lambda^2)[&\eta_1(\bar{\nu}_{\mu L}\gamma^\kappa\mu_L)(\bar{e}_L\gamma_\kappa\nu_{eL}) + \eta_2(\bar{\nu}_{\mu R}\gamma^\kappa\mu_R)(\bar{e}_R\gamma_\kappa\nu_{eR}) \\ &+ \eta_3(\bar{\nu}_{\mu L}\gamma^\kappa\nu_{eL})(\bar{e}_R\gamma_\kappa\mu_R) + \eta_4(\bar{e}_L\gamma_\kappa\mu_L)(\bar{\nu}_{\mu R}\gamma^\kappa\nu_{eR}) \\ &+ \eta_5(\bar{\nu}_{\mu L}\mu_R)(\bar{e}_L\nu_{eR}) + \eta_6(\bar{\nu}_{\mu L}\nu_{eR})(\bar{e}_L\mu_R) \\ &+ \eta_7(\bar{\nu}_{\mu R}\mu_L)(\bar{e}_R\nu_{eL}) + \eta_8(\bar{\nu}_{\mu R}\nu_{eL})(\bar{e}_R\mu_L) \end{aligned} \tag{6}$$

where g is a coupling of hadronic strength; the η_i are of order unity and are normalized so that $|\eta_L| = 1$ in the diagonal coupling

$$(g^2/2\Lambda^2)[\eta_L(\bar{e}_L\gamma^\kappa e_L)(\bar{e}_L\gamma_\kappa e_L) + \cdots].$$

The first and second terms in (6) are purely left-handed and right-handed respectively and hence are indistinguishable from the usual (V-A) and (V+A) interactions.

There are three special cases of interest:

1. If only left-handed (right-handed) leptons are composite, then only the purely left-handed (right-handed) term survives, i.e. only $n_1(\eta_2) \neq 0$.
2. If both left-handed and right-handed leptons are composite but contain quite different sets of constituents, then the purely left-handed and right-handed terms dominate, i.e. $\eta_1, \eta_2 \gg$ other η_i.
3. If there is no ν_R, or $M(\nu_R)$ is very large, only $\eta_1, \eta_3 \neq 0$.

Assuming an effective interaction Lagrangian

$$L_{eff} = L_{V-A} + L_{cont}$$

we obtain the end point decay rate

$$1 - \frac{\xi P\delta}{\rho} = 2(620\ \text{GeV}/\Lambda)^4(g^2/4\pi)^2(\eta_2^2 + \eta_3^2 + \eta_5^2/4) \tag{7}$$

Our limit $1 - \xi P_\mu\delta/\rho < 0.0034$ then implies

$$\Lambda^2 > (3050\ \text{GeV})^2(g^2/4\pi)\sqrt{(\eta_2^2 + \eta_3^2 + \eta_5^2/4)}$$

with 90% confidence. (If the not unreasonable assumptions $g^2/4\pi \approx 2.1$ and $n_i > 0.2$ are

made, the limit $\Lambda > 2400$ GeV would be obtained.)

For the special cases discussed earlier the limit becomes

1. Only left-handed leptons composite: no limit
2. Left and right-handed leptons have different sets of constituents: $\Lambda^2 > (3050\ \mathrm{GeV})^2(g^2/4\pi)\eta_2$
3. No ν_R, or $M(\nu_R)$ very large: $\Lambda^2 > (3050\ \mathrm{GeV})^2(g^2/4\pi)\eta_3$

This work was supported by the Director, Office of Energy Research, Office of High Energy and Nuclear Physics, Division of High Energy Physics of the U. S. Department of Energy under contract #DC-AC03-76SF00098.

References

1. S. L. Glashow, Nucl. Phys. *22*, 579 (1961).
2. S. Weinberg, Phys. Rev. Lett. *19*, 1264 (1967).
3. A. Salam, Proc. 8th Nobel Symposium, Aspenäsgården (Almqvist and Wiksell, Stockholm, 1968), p. 367.
4. J. C. Pati and A. Salam, Phys. Rev. Lett. *31*, 661 (1973) and Phys. Rev. *D10*, 275 (1974);
   R. N. Mohapatra and J. C. Pati, Phys. Rev. *D11*, 566 and 2588 (1975).
5. M. A. B. Beg et al., Phys. Rev. Lett. *38*, 1252 (1977).
6. B. R. Holstein and S. B. Treiman, Phys. Rev. D16, 2369 (1977).
7. G. Beall, M. Bander and A. Soni, Phys. Rev. Lett. *48*, 848 (1982).
8. P. DeForcrand, Ph.D. Thesis, Univ. of Calif., Berkeley (1982), LBL-14692.
9. R. N. Mohapatra et al., Phys. Rev. *D28*, 546 (1983).
10. M. Denis, Phys. Rev. *D28*, 1219 (1983).

11. J. Donoghue and B. R. Holstein, Phys. Lett. *113B*, 382 (1982).

12. The primary input to the world average is V. V. Akhmanov et al., Yad. Fiz. *6*, 316 (1967).

13. The primary input to the world average is J. Peoples, Nevis Cyclotron Report No. 147 (1966).

14. J. Van Klinken, Nucl. Phys. *75*, 145 (1966).

15. J. Van Klinken et al., Phys. Rev. Lett. *50*, 94 (1983).

16. D. Schreiber and F. T. Calaprice, private communication;
D. Schreiber, Ph.D. Thesis, Princeton University, 1983 (unpublished). We calculated the contour plotted in Fig. 1 using A(0) = 0.0363 ± 0.0008; ft ratio = 1.797 ± 0.002. See also F.T. Calaprice et al., Phys. Rev. Lett. *35*, 1566 (1975).

17. H. Abramowicz et al., Z. Phys. *C12*, 225 (1982).

18. V. V. Akhmanov, I. I. Gurevich, Yu. P. Dobretsov, L. A. Makar'ina, A. P. Mishakova, B. A. Nikol'skii, B. V. Sokolov, L. V. Surkova, and V. D. Shestakov, Yad. Fiz. *6*, 316 (1967) (Sov. J. Nucl. Phys. *6*, 230 (1968)).

19. A. E. Pifer et al., Nucl. Instrum. Methods *135*, 39 (1976).

20. C. J. Oram et al., Nucl. Instrum. Methods *179*, 95 (1981).

21. J. Carr et al., Phys. Rev. Lett., *51*, 627 (1983).

22. D. Fryberger et al., Phys. Rev., *166*, 1379 (1968).

23. K. Mursula et al., Nucl. Phys. *B219*, 321 (1983).

24. F. Wilczek, Phys. Rev. Lett. *49, 1549 (1982).*

25. M. Abolins et al., Proc. 1982 DPF Summer Study Elem. Part. Phys. and Future Facilities (Snowmass, 1982), p. 274.

26. E. J. Eichten et al., Phys. Rev. Lett. *50*, 811 (1983).

27. M. E. Peskin, private communication.

28. K. D. Lane and E. Barany, private communication.

Figure Captions

Fig. 1. Experimental 90% confidence limits on the $W_{L,R}$ mass-squared ratio α and mixing angle ζ. The allowed regions are those which include $\alpha = \zeta = 0$. Muon-decay contours are derived from the polarization parameter ξP_μ (dotted, Ref. 12); and the Michel parameter ρ (solid, Ref. 13). Nuclear β-decay contours are obtained from the Gamow-Teller β polarization (dot-dashed, Ref. 14); the comparison of Gamow-Teller and Fermi β polarization (long-dashed, Ref. 15); and the ^{19}Ne asymmetry A(0) and ft ratio, assuming CVC (short-dashed, Ref. 16). Limits from the y distributions in νN and $\bar{\nu}$N scattering (double lines, Ref. 17), are valid irrespective of the ν_R mass. The small bold contour represents the present result.

Fig. 2. Positron momentum spectrum from completely polarized μ^+ decay at rest in the direction opposite to the muon spin for V-A and V+A interactions. Also shown is the spectrum from unpolarized μ^+ decays. The effects of internal radiation corrections are indicated. The apparatus acceptance is denoted by the thick portion of the V-A curve.

Fig. 3. Particle fluxes in the M13 beam at TRIUMF. The μ^+ with momenta corresponding to the sharp (surface muon) edge at 29.5 MeV/c are those produced by π^+ decay near the surface of the production target. Those with smaller momenta are from π^+ decay deeper in the production target, and are less polarized. Muons with momenta above the edge are from π^+ decay deeper in the production target, and are less polarized. Muons with momenta above the edge are from π^+ decay in flight near the production target.

Fig. 4. Plan view of the muon polarimeter. P1-P3 are proportional wire chambers, D1-D4 are drift chambers, and S1-S3 are scintillators. The trigger is T1·T2, where T1 is $P1 \cdot S1 \cdot P2 \cdot \overline{V1} \cdot \overline{P3} \cdot \overline{S2}$ at the μ^+ stopping time, T2 is $P3 \cdot S2 \cdot S3 \cdot \overline{P1} \cdot \overline{S1} \cdot \overline{V1} \cdot \overline{P2} \cdot \overline{V2}$ at the μ^+ decay time, and V1 and V2 are veto scintillators surrounding S1 and S2 respectively (not shown).

Fig. 5. Distributions (uncorrected for acceptance) in reduced positron momentum with the μ^+ spin (a) precessed and (b) held. The indicated errors are statistical. The edge in (a) corresponds to a resolution with a gaussian part <0.2% rms. The fits are described in the text.

Fig. 6. The fitted values of $(\xi P_\mu \delta/\rho)\langle\cos\vartheta\rangle$ tor data in each of five bins in $\cos\vartheta$. The errors are statistical. A fixed slope extrapolation to $\cos\vartheta = 1$ is made to determine $\xi P_\mu \delta/\rho$.

Fig. 7. The fitted values of $\xi P_\mu \delta/\rho$ for each of the four stopping target materials.

Fig. 8. The time spectrum of the spin-precessed data, after removal of the muon life-time dependence, shown together with the maximum likelihood fit. The ordinate scale is arbitrary. The non-zero values of the amplitude at the minima are a consequence of the fact that the data were taken with finite momentum and angular acceptance.

Fig. 9. Values of $\frac{\xi P_\mu \delta}{\rho}$ obtained with the μSR method for various targets and precessing fields: (1) Au240 mg/cm^2, 70 Gauss (2) Au240 mg/cm^2, 120 Gauss (3) Al 150 mg/cm^2, 70 Gauss (4) Al 150 mg/cm^2, 120 Gauss (5) Al 280 mg/cm^2, 120 Gauss (6) Cu160 mg/cm^2, 70 Gauss (7) Cu160 mg/cm^2, 120 Gauss (8) Cu220 mg/cm^2, 120 Gauss

Fig. 10. The decay asymmetry for the spin-precessed data as a function of reduced positron momentum. The curve shown is that expected for $\delta = 3/4$ with radiative corrections.

Fig. 11. Comparison of the results of this experiment with the previous world-average.

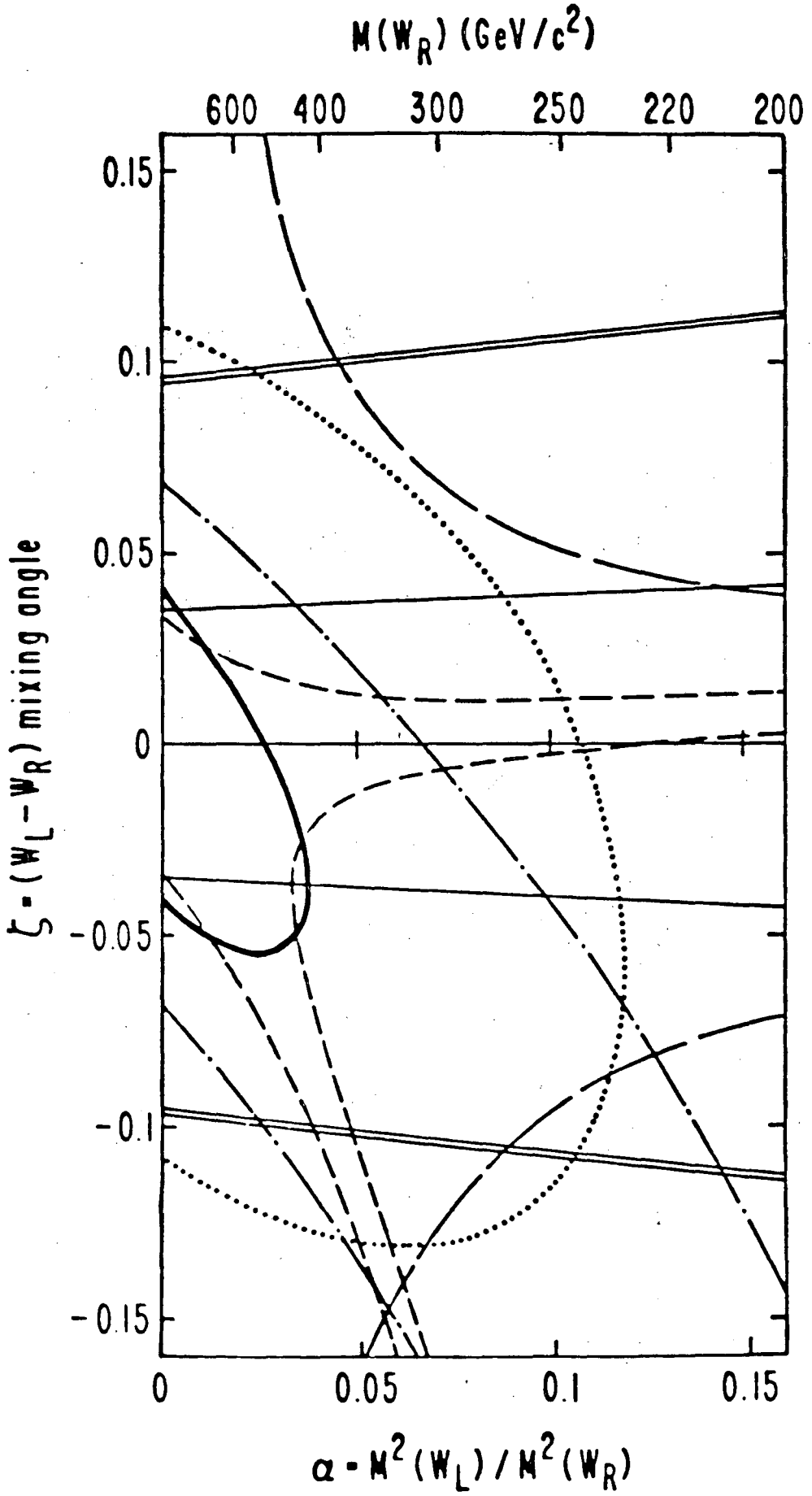
M(W_R) (GeV/c²)
600
400
300
250
220
200
0.15
0.1
0.05
0
-0.05
-0.1
-0.15
ζ = (W_L - W_R) mixing angle
0
0.05
0.1
0.15
α = M²(W_L)/M²(W_R)

Figure 1

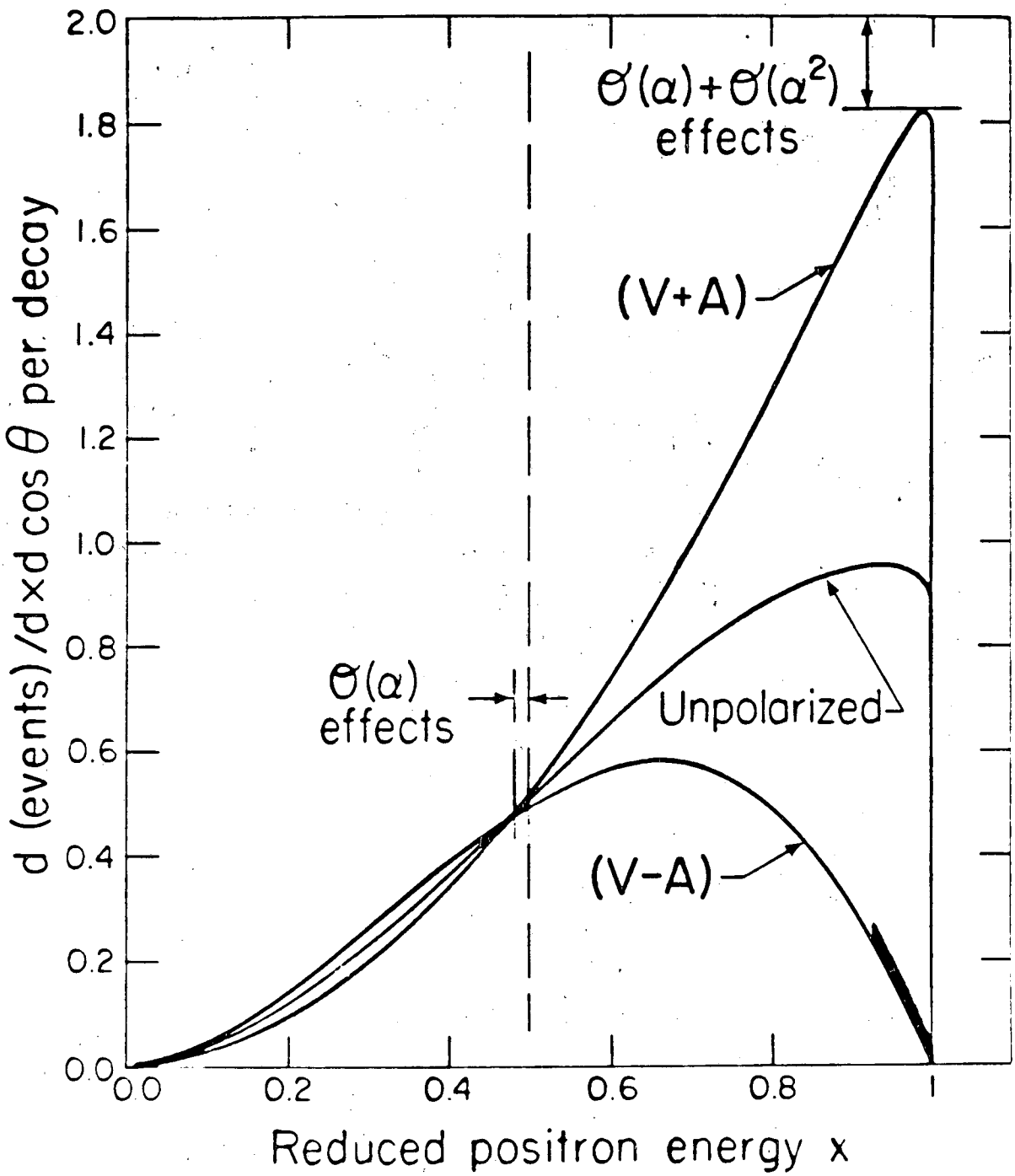

XBL 811-2103

Figure 2

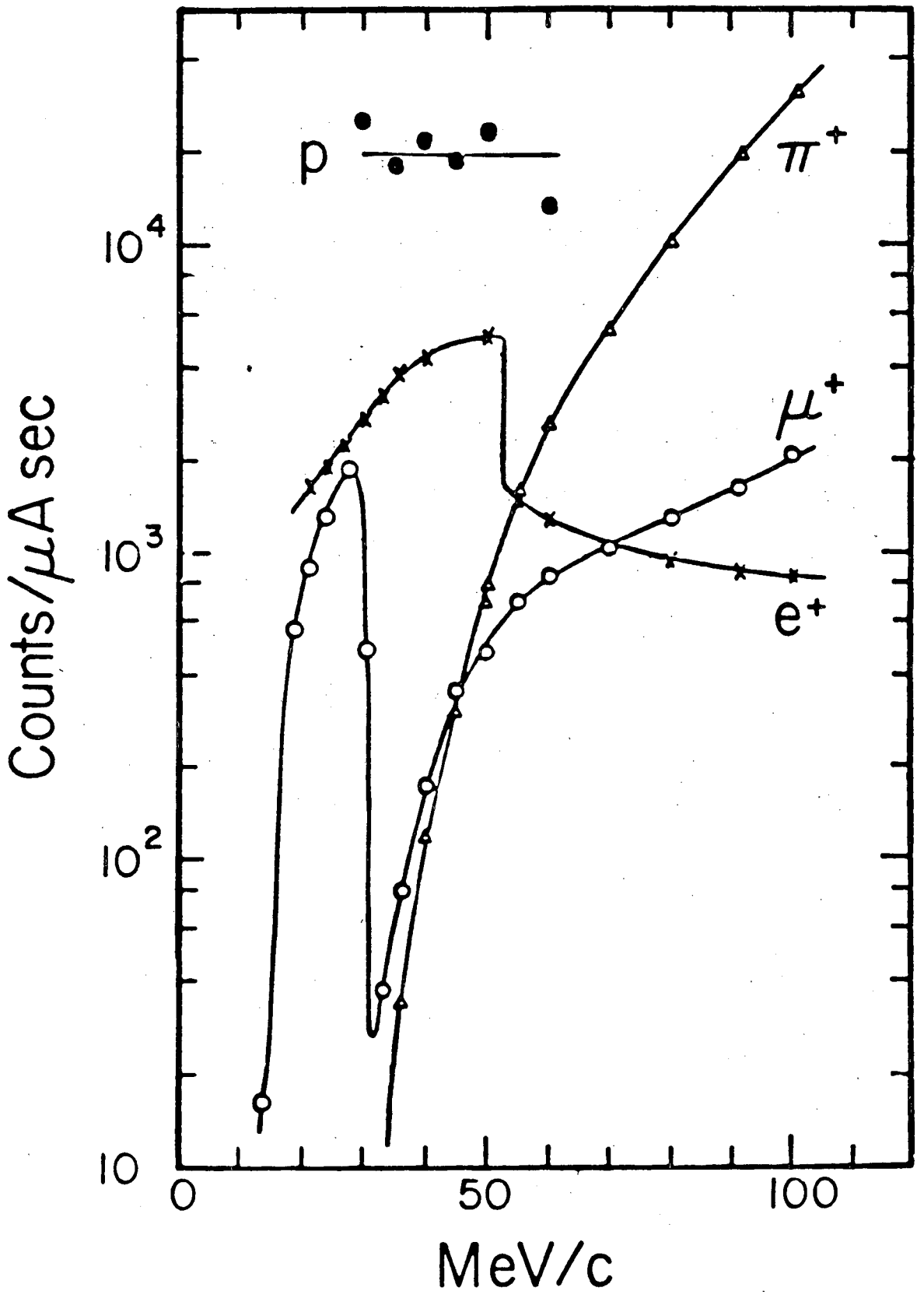

Figure 3

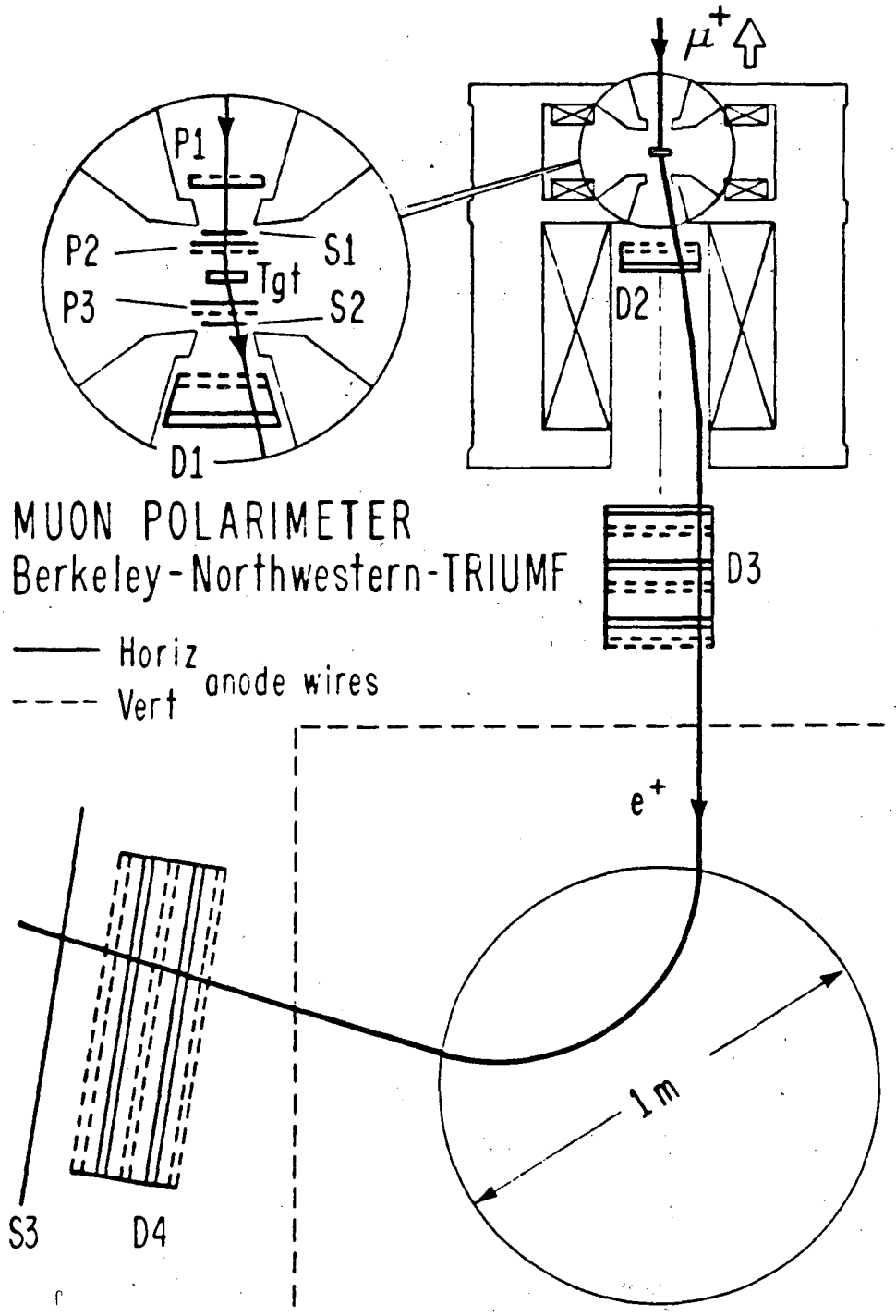

XBL 834 147

Figure 4

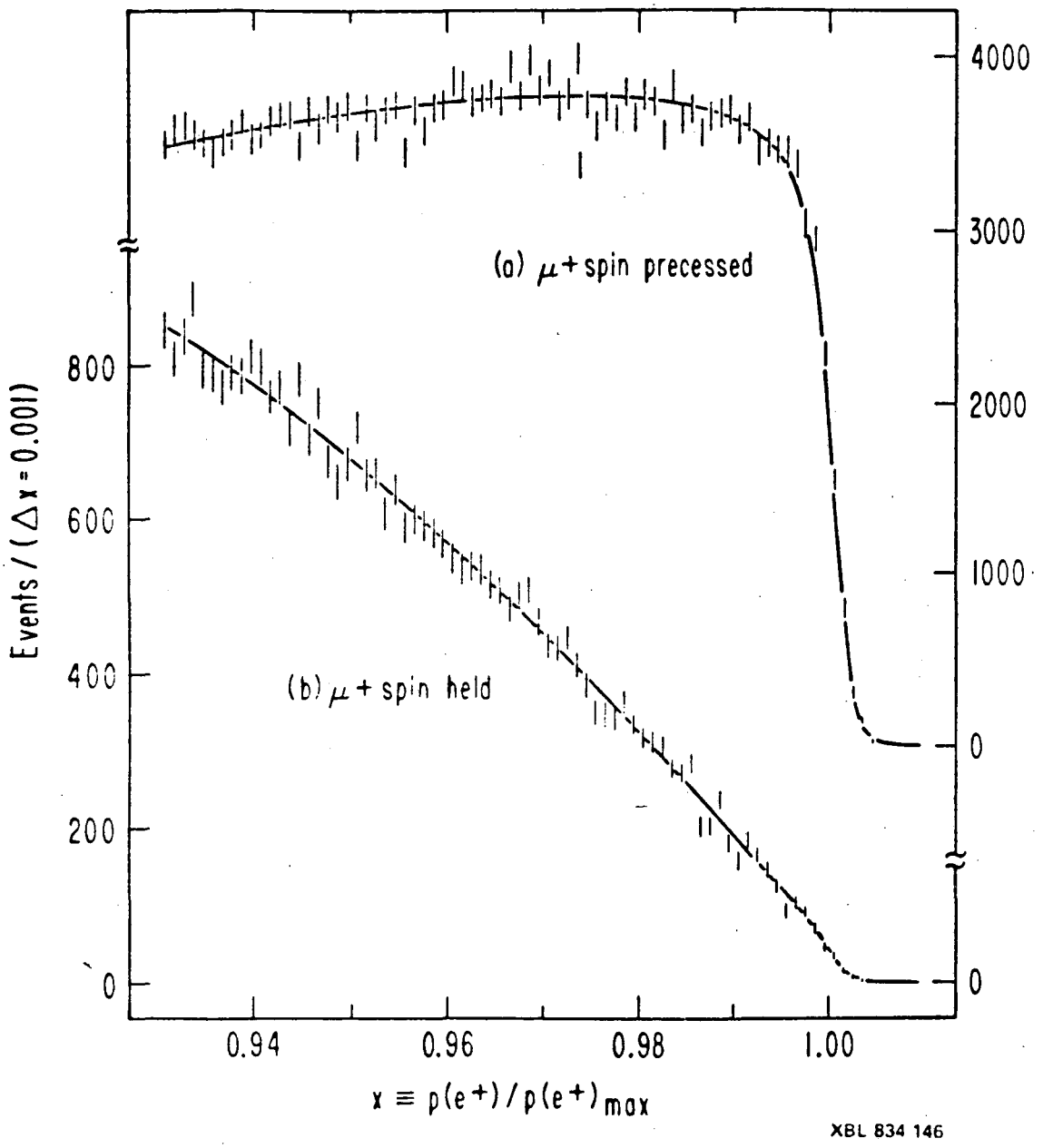
(a) μ+ spin precessed
(b) μ+ spin held
Events / (Δx = 0.001)
800
600
400
200
0
4000
3000
2000
1000
0
0
0.94
0.96
0.98
1.00
x ≡ p(e+)/p(e+)max
XBL 834 146

Figure 5

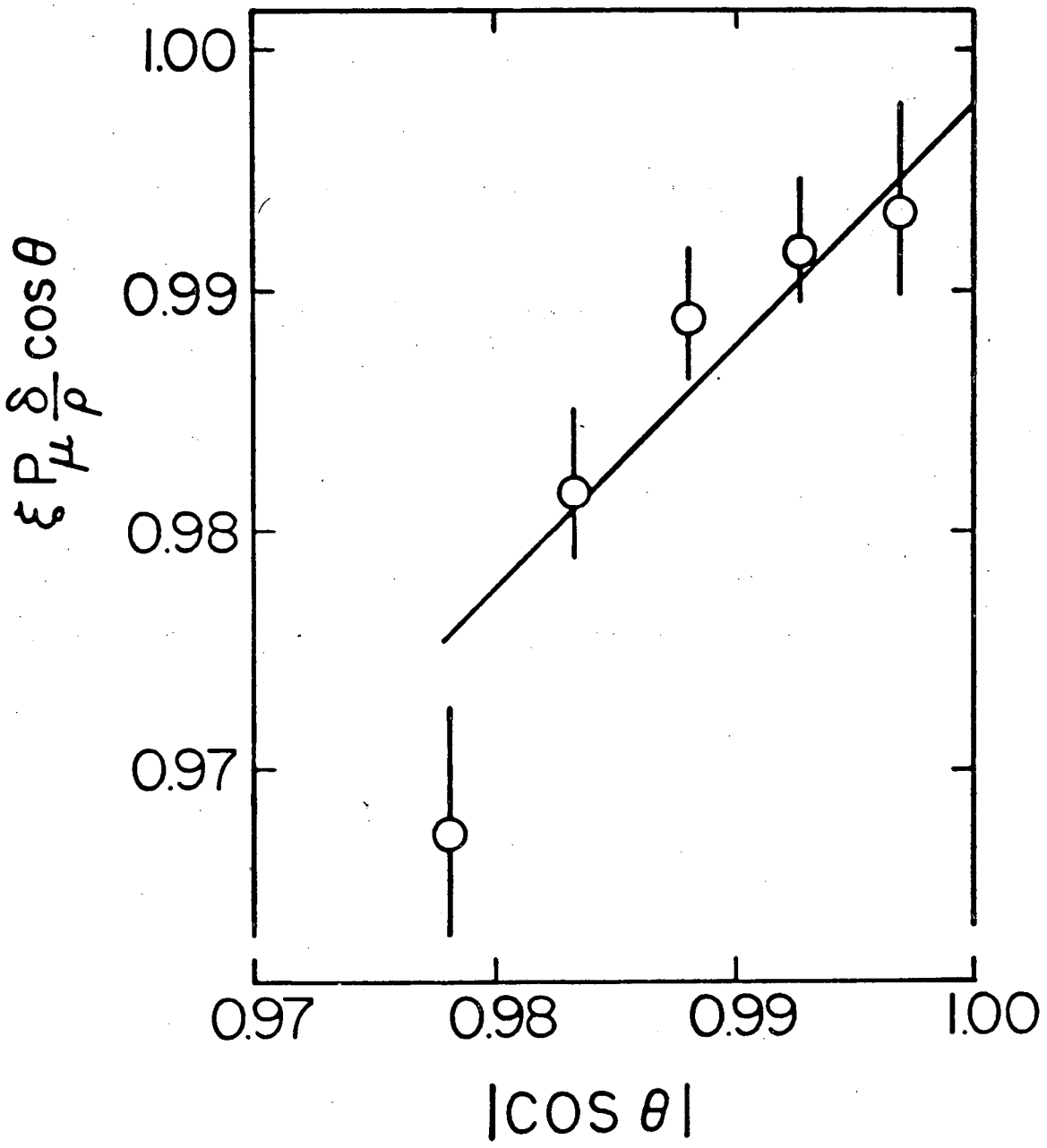
1.00
0.99
0.98
0.97
$\xi P_\mu \frac{\delta}{p} \cos\theta$
0.97
0.98
0.99
1.00
$|\cos\theta|$

Figure 6

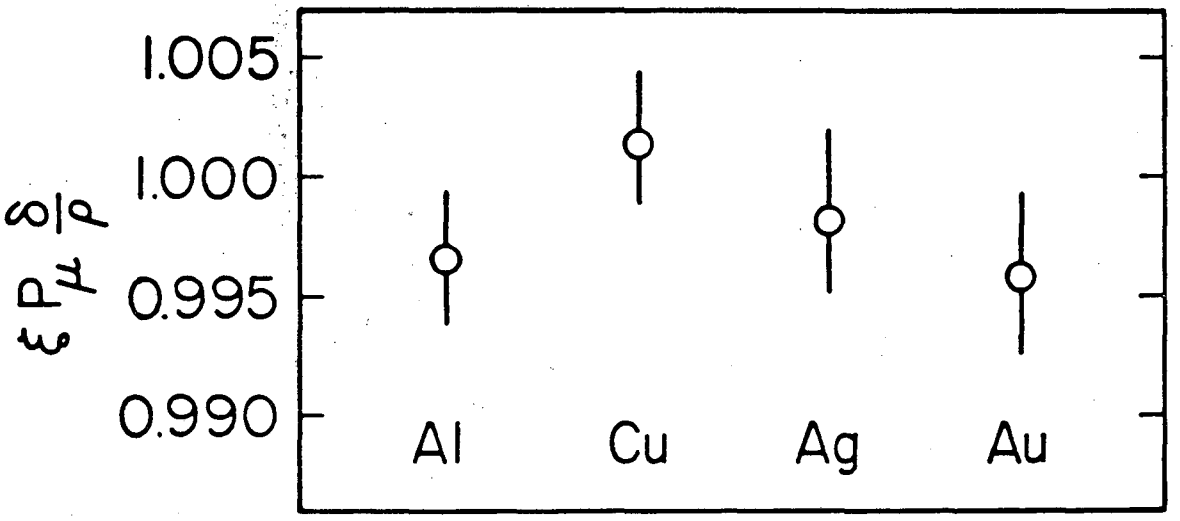

Figure 7

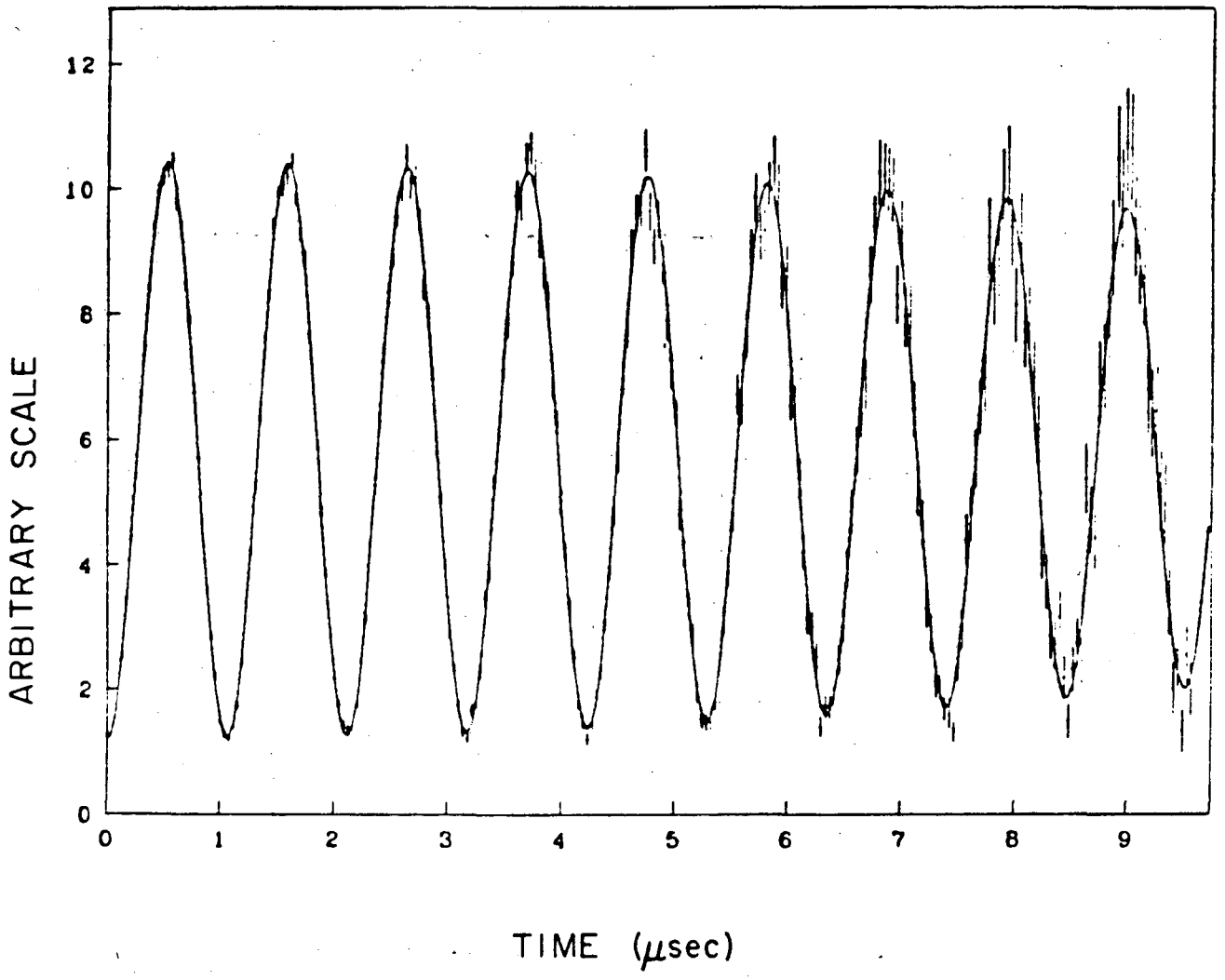

Figure 8

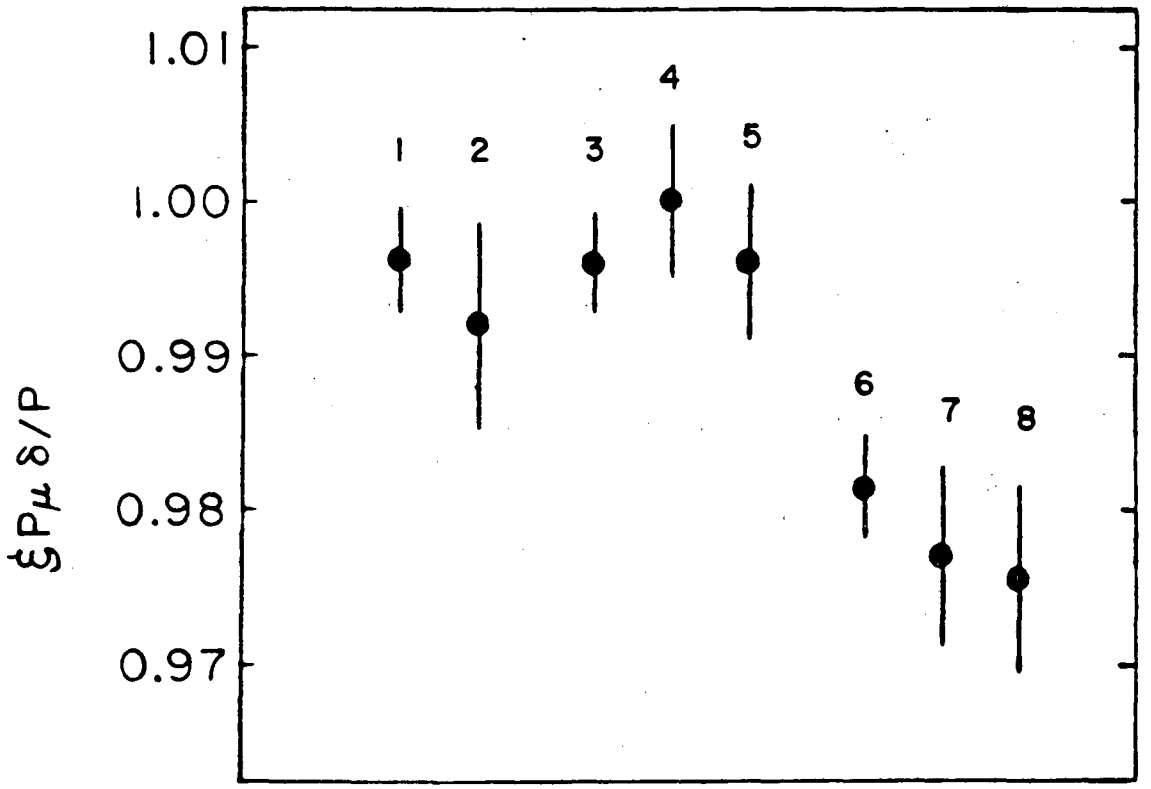

Figure 9

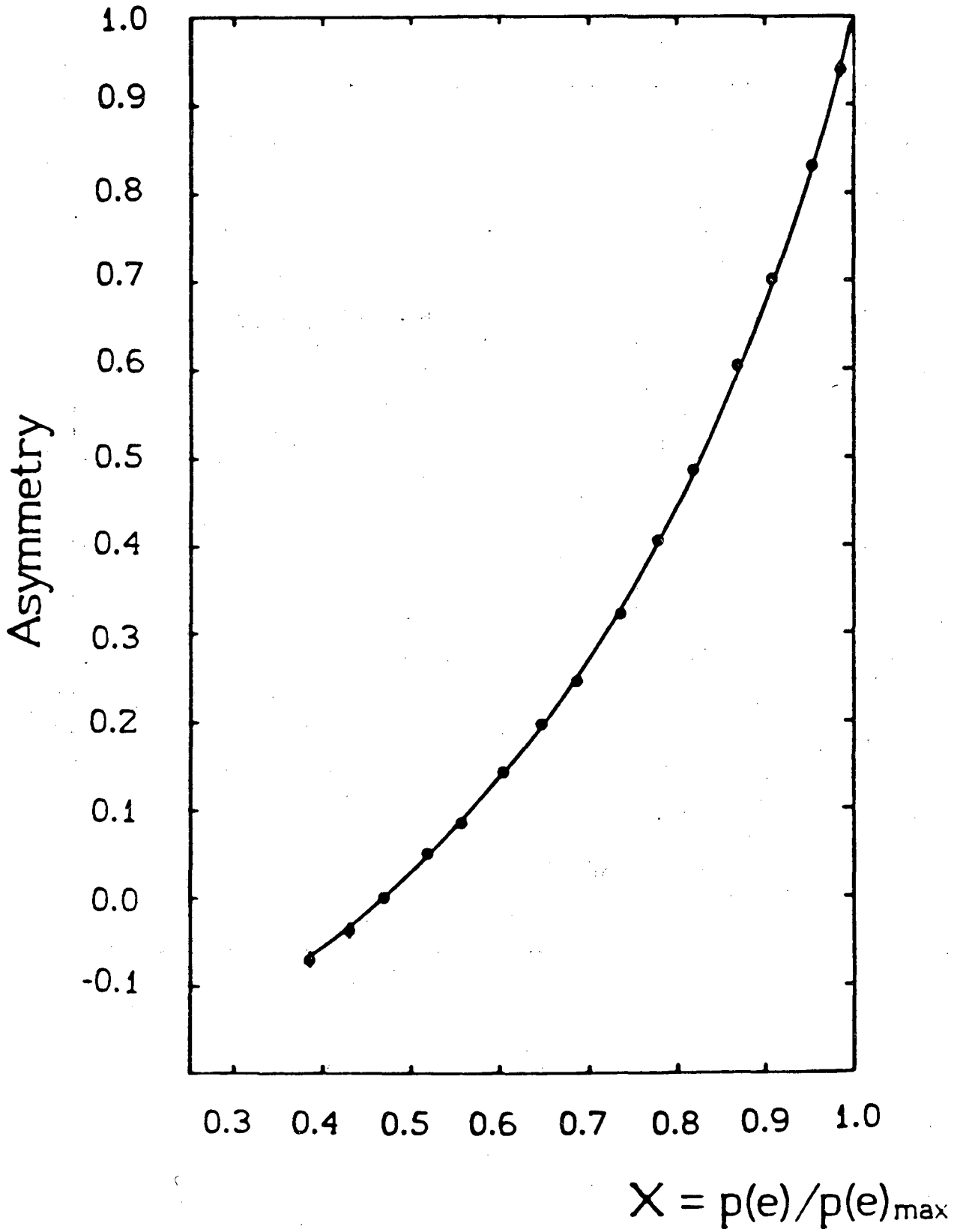
1.0
0.9
0.8
0.7
0.6
0.5
0.4
0.3
0.2
0.1
0.0
-0.1
Asymmetry
0.3
0.4
0.5
0.6
0.7
0.8
0.9
1.0
X = p(e)/p(e)max

Figure 10

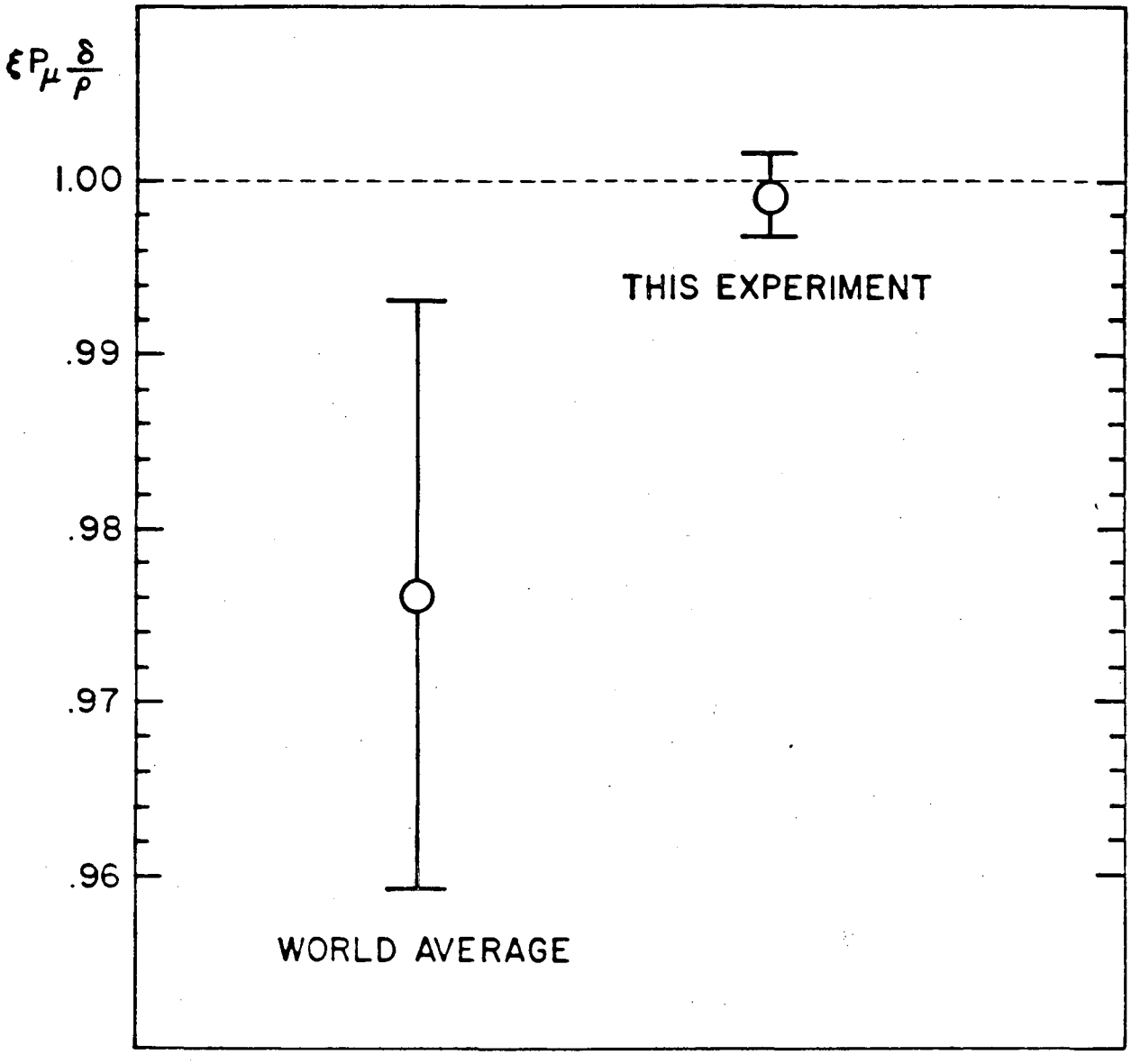
$\xi P_\mu \frac{\delta}{\rho}$
1.00
.99
.98
.97
.96
THIS EXPERIMENT
WORLD AVERAGE

Figure 11

This report was done with support from the Department of Energy. Any conclusions or opinions expressed in this report represent solely those of the author(s) and not necessarily those of The Regents of the University of California, the Lawrence Berkeley Laboratory or the Department of Energy.

Reference to a company or product name does not imply approval or recommendation of the product by the University of California or the U.S. Department of Energy to the exclusion of others that may be suitable.

TECHNICAL INFORMATION DEPARTMENT
LAWRENCE BERKELEY LABORATORY
UNIVERSITY OF CALIFORNIA
BERKELEY, CALIFORNIA 94720